SIMPLE LASER-DRIVEN, METAL PHOTOCATHODES* AS COLD, HIGH-CURRENT ELECTRON SOURCES

J. D. Saunders and T. J. Ringler
Naval Postgraduate School
Monterey, California 93943

L. A. Builta, T. J. Kauppila, and D. C. Moir
Los Alamos National Laboratory
P.O. Box 1663
Los Alamos, New Mexico 87545

S. W. Downey
AT&T Bell Laboratories
Murray Hill, NJ 07974

Abstract

Recent developments in excimer laser design have made near ultraviolet light intensities of several MW/cm^2 possible in unfocused beams. These advances and recent experiments indicate that high-current, simple-metal photoemissive electron guns are now feasible. Producing more than 50 A/cm^2 of illuminated cathode surface, the guns could operate at vacuums of 10^{-6} torr with no complicated system components inside the vacuum enclosure. The electron beam produced by such photoemission guns would have very low emittance and high brightness. This beam would also closely follow the temporal characteristics of the laser pulse, making fast risetime, ultrashort electron beam pulses possible.

Introduction

This paper presents the results of recent experiments conducted on a simple-metal photocathode electron gun.[1,2] Parameters were measured for calculational estimates of total current, current density, emittance, brightness, and the practical quantum yield relevant to simple-metal, high-current, and high-voltage photocathode electron guns. The source could have application for a PHERMEX injector[3] or a diode-type, pulse-power, flash radiographic source.

Experimental Technique

A Questek Model 2000 KrF excimer laser was the photon source. The excimer laser produces a photon energy of 5 eV at a wavelength of 248 nm and with a full pulse width of 30 ns. Figure 1 shows the laser light path components.

Laser light at 100 mJ per pulse in a 3-cm^2 beam cross section was apertured to 0.4 cm^2 and then passed through a "laser variable attenuator," Newport Research Corporation Model 935-10. The attenuated beam was then transported through an uncoated Suprasil quartz window and apertured to a 0.18-cm^2 cross section in the vacuum chamber. After the final aperture, the beam illuminated the cathode at a 45° incident angle. The laser light reflected from the quartz vacuum window to the photodiode (Hamamatsu R1193U-04) was used as a relative, time-resolved monitor of the laser output intensity.

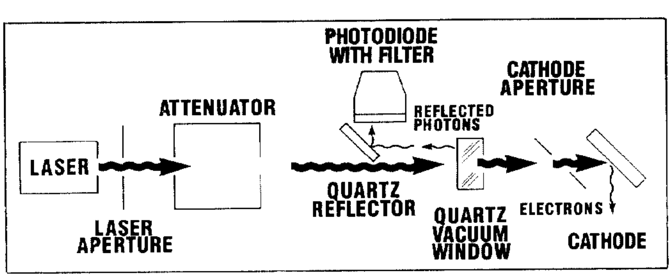

Fig. 1. Light path components.

A removable metal cathode disc, 2.5 cm in diameter and 0.4-cm thick, was attached to a high-voltage connector inside the vacuum chamber wall. Prior to installation the cathode was polished in air to a surface roughness of about 10 μm. When in place, the cathode was centered in front of and parallel to an aluminum anode of the same diameter. Figure 2 illustrates the physical anode-cathode (A-K) arrangement. The A-K gap was 18.5 mm, and the accelerating potential across the gap was variable from 0 to 30 kV. Photoelectrons emitted from the 0.18-cm^2 spot illuminated by the laser were accelerated toward the anode. The subsequent beam was collimated by the 0.071-cm^2 opening at the center of the anode. The transmitted electrons then were collected on an aluminum wire collector that ran parallel to the electron beam axis. The collector, with a cross-sectional area of 0.156 cm^2, was the center conductor of a 50-Ω coaxial cable. The purpose of the aperture was to eliminate the electric field from the surface of the collector. The anode and all other portions of the vacuum chamber and support hardware were at ground potential.

Three parameters monitored during data acquisition were laser energy, A-K voltage, and the photoelectron current. The photodiode driven by reflected laser light was used as the trigger source for all analyzing equipment. One oscilloscope was dedicated to monitoring this pulse. The second oscilloscope was used as the collector voltage monitor or the calibrating joulemeter monitor, as appropriate. All oscilloscopes were 2-GHz Tektronix Model 7103. Data acquisition was primarily by oscilloscope photographs.

The vacuum system consisted of a vacuum chamber with a volume of approximately 10 ℓ. This chamber was neoprene o-ring sealed and pumped by a Cryogenics Cryo-torr-8 cryopump. The best vacuum achieved was 8×10^{-8} torr after 12 hours of pumping. Most data were acquired with a vacuum of about 10^{-6} torr. Because the nature of the experiment required frequent adjustments inside the vacuum boundary with no remote manipulation ability, the vacuum boundary was frequently broken.

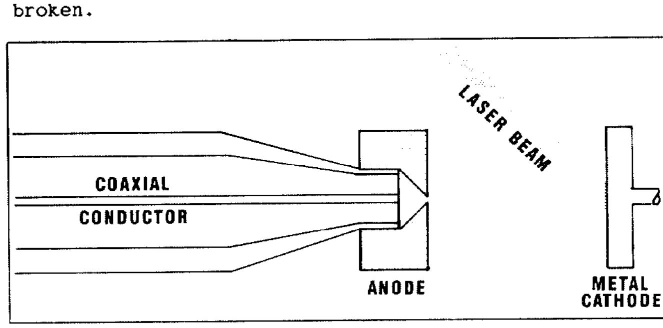

Fig. 2. Anode/cathode arrangement.

*Work performed under the auspices of the U.S. Department of Energy by Los Alamos National Laboratory under W-7405-ENG-36.

CH2387-9/87/0000-0337 $1.00 © 1987 IEEE
PAC 1987

Data Acquisition and Reduction Techniques

Four experimental apparatus limitations dictated the scope of the data. The accelerating potential electrical connection to the cathode was rated at 25-kV standoff and could not be relied upon to hold off breakdown above 28 kV. In addition, the minimum A-K gap achievable was 1.8 cm, resulting in a maximum field of less than 15 kV/cm. The current collector electrical system had an inherent noise level that tended to chop and distort the current pulse signal for collector currents below about 0.7 mA. Accurate measurement of laser intensity at low power levels was not possible with the joulemeter. Therefore, the laser's energy was determined using the fast response photodiode calibrated, in situ, with a Gentec-200 calorimeter head.

The fast photodiode output variance with laser pulse energy was nonlinear. A photodiode output voltage (V) vs joulemeter energy (E) calibration curve was obtained just prior to data acquisition. The photocathode was removed and a joulemeter placed in the location of the cathode disc. The laser was pulsed and the outputs of the joulemeter and the photodiode were simultaneously monitored. The data were found to fit the relation

$$E = 0.0046\ V^{6.16} \quad , \tag{1}$$

where V is in volts and E is in mJ per pulse. The joulemeter value is time integrated whereas the peak photodiode voltage is measured at a single time. A least squares fit of the time integral of the photodiode voltage vs the peak photodiode voltage yielded the following relationship,

$$V_{peak} = c\left[\int_{pulse} V(t)dt\right]^{0.52} \quad . \tag{2}$$

Even though the peak voltage is an adequate representation of the total energy, it is not optimum because small errors in the peak measurement produce large errors in the laser energy. The cube of the integral of the voltage is proportional to the energy. This is less sensitive to errors than the peak. The dependence of the laser energy on the photodiode voltage and integrated voltage is obviously nonlinear. This dependence is not understood. The overall statistical uncertainty was minimized by averaging 20 successive pulses.

The maximum current was limited by Child-Langmuir flow.[4] The current density is given by,

$$J = PV^{3/2}\ d^{-2} \quad , \tag{3}$$

where d is the A-K spacing (cm), V the potential (V), and P the perveance of a planar geometry (2.34×10^{-6} $AV^{-3/2}$).[5] This expression is for an infinitely large planar A-K geometry and does not precisely represent a cylindrical beam. However, it is a reasonable approximation and is useful in interpreting the data. This space-charge limited electron flow was an important upper data bound in determining quantum efficiencies.

An estimate of beam emittance was made by replacing the anode apparatus with one that employed two parallel flat disc plates with apertures in each. The apertures were colinear with the charge collector. The first disc served as an anode aperture; the second disc was a collimator. The disc-to-disc spacing was 2.5 times the window diameter. Operating at 20-kV accelerating potential, the laser-illuminated zinc cathode emitted electrons. The distance from the collector to the collimating disc was varied to obtain information on beam divergence.

Results

Data obtained at two different laser intensities with varying electric field strength applied to a Zn photocathode are shown in Fig. 3. As expected, the low field data are limited by the Child-Langmuir space-charge limited flow. The quantum yield does not increase as the applied electric field increases. In fact, the quantum yield and current are maximized in the low field region and then peak again at about 13 kV/cm, with the high field portion of the curve apparently approaching some lower constant value. Increasing the laser intensity by a factor of two increased the quantum yield and shifted the peaks to higher field values.

The emittance was calculated using the extrapolated 50% current loss drift distance. The beam is assumed to be uniform in the plane transverse to the beam axis. The resulting normalized emittance (ϵ_n) is 0.83 π mrad x mm. This normalized emittance value corresponds to a transverse beam energy of 2.2 eV. The electrons in the beam would have an equivalent temperature of 2.5×10^4 K.

The data for peak photoelectron current density of Zn versus power are displayed in Fig. 4. As discussed earlier, the power is obtained from the photodiode calibration of the energy. This energy is divided by the time of the laser pulse to obtain power. The current density is obtained directly from the current measurement by the charge collector divided by the measured area of the anode aperture. Figure 4 demonstrates that the current is not a linear function of power. In fact, below the space-charge limit the curve shows current to be a quadratic function of power. This result will be discussed in detail later. Another observation is that the maximum current is well correlated to the 2.1 A/cm^2 value predicted for space-charge limited flow between parallel plates. All other metals showed similar behavior for space-charge limited flow except Al, which will be discussed later.

The Zn quantum yields, uncorrected for reflectance, are plotted in Fig. 5. The quantum efficiency, QE, is given by

$$QE = \text{Current density } (A/cm^2)/\text{Power } (W/cm^2) \times 5\ eV/photon \quad . \tag{4}$$

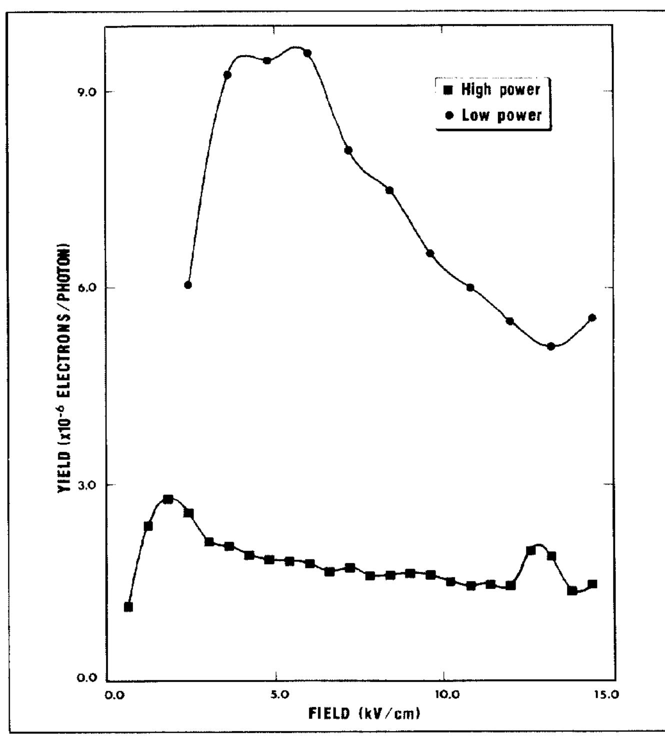

Fig. 3. Quantum efficiency vs electric field.

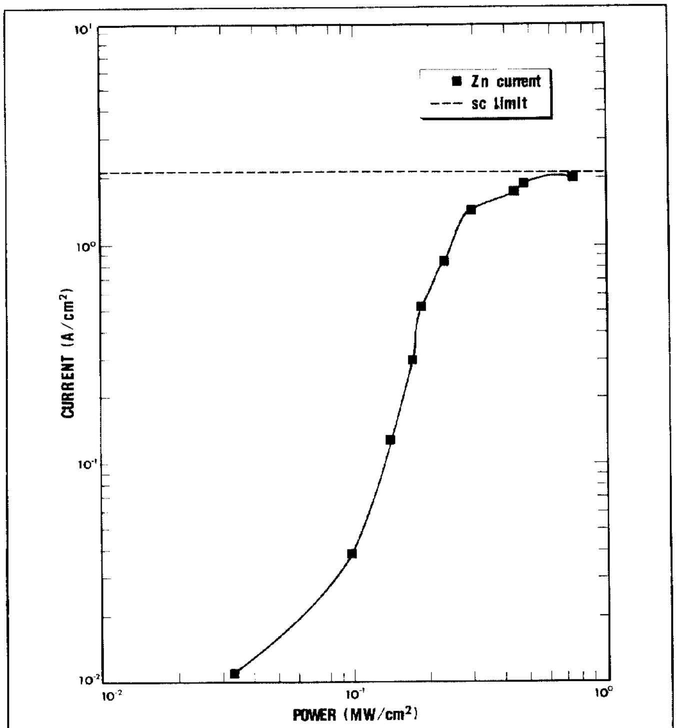

Fig. 4. Variance in the current density (A/cm^2) as a function of incident laser power (MW/cm^2).

At the space-charge limit the current density is constant and independent of power. Therefore, the line indicating the space-charge limit is given by

$$QE \propto (1/Power) \quad . \tag{5}$$

Again the data near the space-charge limit behave as expected. At lower power, less than 0.1 MW/cm^2, data show a near constant quantum yield. These data are

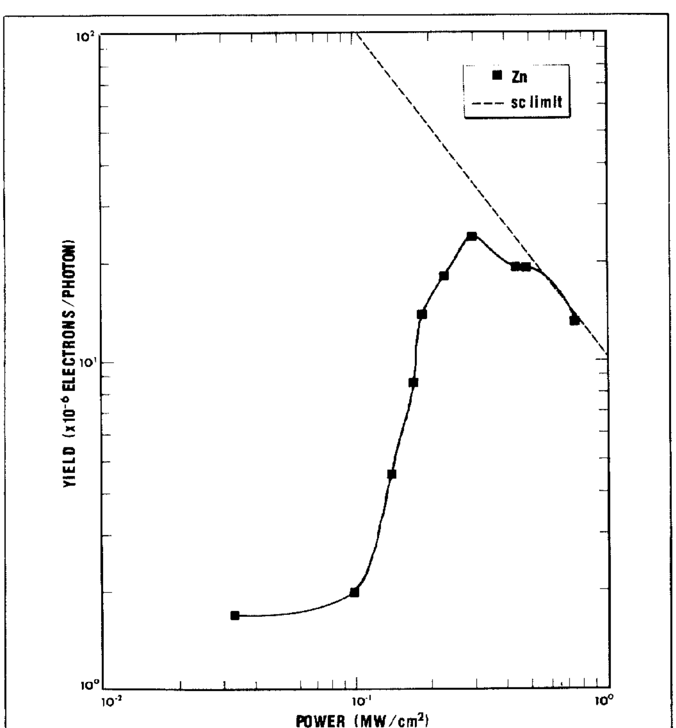

Fig. 5. Quantum yield (electrons/photon) vs light intensity (MW/cm^2).

well above the minimum detection threshold of the system. This is believed to be a result of a single photon generating a photoelectron. At laser powers greater than 0.1 MW/cm^2, the quantum efficiency increases quadratically. The most probable explanation is that the electrons are produced by a two-photon process.

A review of the data for other metals shows Ni has the lowest uncorrected quantum yield (5.9×10^{-6} electrons/photon) and Pb has the highest (1.3×10^{-4} electrons/photon). However, both reached the space-charge limit prior to attaining a constant quantum yield, so significantly higher quantum yields may be possible.

Conclusion

In summary, the simple-metal, photocathode electron gun operating at 10^{-6} torr and a maximum of 1 MW/cm^2 of 248-nm light intensity and at fields of 12 kV/cm produced current densities beyond 2 A/cm^2 in the space-charge limit. This arrangement was useful for obtaining relative quantum efficiencies for various metals. The space-charge limit prevents observation of the maximum quantum efficiency at full laser power. Therefore, in order to obtain quantum efficiencies at high power, these results must be extrapolated. If the near quadratic dependence of η on power holds, quantum efficiencies greater than 3×10^{-3} electrons/photon might be achieved. However, even at the quantum yields established here, a 5-MW/cm^2, 248-nm intensity could produce over 23 A/cm^2 from Zn. In addition, that same current density can be produced from Pb at 1 MW/cm^2. An 80-cm^2 cathode (area of PHERMEX electron gun cathode) could be expected to produce a beam current of more than 900 A when driven by a 800-mJ KrF excimer laser.

At present work is directed toward generating an electron beam in a standard electron gun using an 800-mJ KrF laser on an 80-cm^2 cathode. Because the PHERMEX gun has a capability of generating cathode temperature, the possibility of exploring a hybrid source exists.[6]

References

[1] S. W. Downey, L. A. Builta, D. C. Moir, T. J. Ringler, and J. D. Saunders, Appl. Phys. Lett. 49, 15 (1986).

[2] C. H. Lee, P. E. Oettinger, E. R. Pugh, R. Klinkowstein, J. H. Jacob, J. S. Fraser, and R. L. Sheffield, IEEE Trans. Nuc. Sci. NS-32, 3045 (1985).

[3] L. A. Builta, J. C. Elliott, D. C. Moir, T. P. Starke, and C. A. Vecere, "PHERMEX Electron Gun Development," IEEE Trans. Nuc. Sci. NS-30 (4), 2728 (1983).

[4] I. Langmuir, Phys. Rev. 2 (2), 450 (1913).

[5] J. D. Lawson, "The Physics of Charged Particle Beams," Chap. 3 (1978).

[6] T. J. Kauppila, L. A. Builta, J. K. Crutcher, J. C. Elliott, D. C. Moir, "A Pulsed Electron Injector Using a Metal Photocathode Irradiated by an Excimer Laser," in Proc. of the IEEE Part. Acc. Conf., Washington, DC, March 16-19, 1987, published in this issue.